




iTRAQ-based proteomic analysis reveals the molecule mechanism of reducing higher alcohols in Chinese rice wine by nitrogen compensation

Guidong Huang^{1,2,3,4,5†}, Hong Ren^{1,2,3,4,5†}, Ali Wang^{1,2,3,4,5}, Xinran Wan¹, Ziyang Wu¹ and Xianfeng Zhong^{1,2,3,4,5*} 

Abstract

Purpose: Higher alcohol is a by-product of the fermentation of wine, and its content is one of the most important parameters that affect and are used to appraise the final quality of Chinese rice wine. Ammonium compensation is an efficient and convenient method to reduce the content of higher alcohols, but the molecule mechanism is poorly understood. Therefore, an iTRAQ-based proteomic analysis was designed to reveal the proteomic changes of *Saccharomyces cerevisiae* to elucidate the molecular mechanism of ammonium compensation in reducing the content of higher alcohols.

Methods: The iTRAQ proteomic analysis method was used to analyze a blank group and an experimental group with an exogenous addition of 200 mg/L $(\text{NH}_4)_2\text{HPO}_4$ during inoculation. The extracted intracellular proteins were processed by liquid chromatography-mass spectrometry and identified using bioinformatics tools. Real-time quantitative polymerase chain reaction was used to verify the gene expression of differentially expressed proteins.

Results: About 4062 proteins, including 123 upregulated and 88 downregulated proteins, were identified by iTRAQ-based proteomic analysis. GO and KEGG analysis uncovered that significant proteins were concentrated during carbohydrate metabolism, such as carbon metabolism, glyoxylate, and dicarboxylate metabolism, pyruvate metabolism, and the nitrogen metabolism, such as amino acid synthesis and catabolism pathway. In accordance with the trend of differential protein regulation in the central carbon metabolism pathway and the analysis of carbon metabolic flux, a possible regulatory model was proposed and verified, in which ammonium compensation facilitated glucose consumption, regulated metabolic flow direction into tricarboxylic acid, and further led to a decrease in higher alcohols. The results of RT-qPCR confirmed the authenticity of the proteomic analysis results at the level of gene.

(Continued on next page)

* Correspondence: zhongxf81@126.com

†Guidong Huang and Hong Ren contributed equally to this work.

¹Department of Food Science, Foshan University, Foshan 528231, China

²Guangdong Engineering Research Center for Traditional Fermented Food, Foshan 528231, China

Full list of author information is available at the end of the article



© The Author(s). 2020 **Open Access** This article is licensed under a Creative Commons Attribution 4.0 International License, which permits use, sharing, adaptation, distribution and reproduction in any medium or format, as long as you give appropriate credit to the original author(s) and the source, provide a link to the Creative Commons licence, and indicate if changes were made. The images or other third party material in this article are included in the article's Creative Commons licence, unless indicated otherwise in a credit line to the material. If material is not included in the article's Creative Commons licence and your intended use is not permitted by statutory regulation or exceeds the permitted use, you will need to obtain permission directly from the copyright holder. To view a copy of this licence, visit <http://creativecommons.org/licenses/by/4.0/>.

(Continued from previous page)

Conclusion: Ammonium assimilation promoted by ammonium compensation regulated the intracellular carbon metabolism of *S. cerevisiae* and affected the distribution of metabolic flux. The carbon flow that should have gone to the synthesis pathway of higher alcohols was reversed to the TCA cycle, thereby decreasing the content of higher alcohols. These findings may contribute to an improved understanding of the molecular mechanism for the decrease in higher alcohol content through ammonium compensation.

Keywords: Higher alcohols, Proteomics, Ammonium compensation, *Saccharomyces cerevisiae*, iTRAQ

Introduction

Chinese rice wine (CRW), a national unique and traditional wine that has a long history in China, is an alcoholic beverage that is commonly considered to contain molecules with a nutraceutical and pharmaceutical interest, thus attracting a great deal of attention (Xie 2008; Gao et al. 2018; Wang et al. 2020). The final aroma of CRW constitutes of hundreds of flavor-active compounds produced during brewing, including higher alcohols, esters, volatile acids, and aldehydes (Pires et al. 2014). The main higher alcohols that have a relatively high concentration are isoamylol (66.8-299.5 mg/L), isobutanol (73-238.8 mg/L), n-propyl alcohol (24.3-131.4 mg/L), and β -phenethyl alcohol (35.3-103.7 mg/L) during different treatment fermentation processes of CRW (Yuan et al. 2018). CRW has a total higher alcohol content of 205-700 mg/L, is 1.2-fold higher than that of grape wine (260-299 mg/mL), and 4.5-fold higher than that of beer (55-94 mg/mL) (Sun et al. 2020).

Higher alcohols, which are important flavor components, are related to intoxication and hangovers (Fang et al. 2018). Excessive intake of higher alcohol causes a hangover accompanied by nausea and dizziness (Xie et al. 2018). At a concentration above 400 mg/L, higher alcohols influence the flavor and taste of wine, destroying its quality (Stribny et al. 2016; Longo et al. 2020). At or below 300 mg/L, higher alcohols add a complex aroma and a full-bodied taste to wine, thereby optimizing the quality of CRW and harmonizing its organoleptic properties (Zhong et al. 2019). Therefore, the content of higher alcohols affects the quality of CRW and represents one of the important indexes to evaluate the quality of wine (Zheng et al. 2020). An essential step is to moderately lower the content of higher alcohols to maintain the flavor and improve the final quality of CRW.

The main synthesis pathway of higher alcohols is the Ehrlich pathway related to amino acid catabolism and the Harris pathway associated with glycometabolism (El-Dalatony et al. 2019; Rollero et al. 2015; Yan et al. 2017). With ample nitrogen sources, the biosynthesis of higher alcohols is the de novo synthesis of branched-chain amino acid through the Ehrlich pathway by a sequence of reactions that involve transamination of branched-

chain amino acid, decarboxylation, and reduction of α -ketone acids (Pires et al. 2014; Zhong et al. 2019). The amount of higher alcohols produced in the pathway of branched-chain amino acid synthesis pathway (Ehrlich pathway) accounted for 25% of the total amount of higher alcohols (Hazelwood et al. 2008). When nitrogen sources are insufficient, synthetic precursors of higher alcohols mainly come from ketonic acids, which are largely synthesized from carbohydrate metabolic pathways such as the Embden-Meyerhof-Parnas pathway (EMP) and tricarboxylic acid cycle (TCA), accounting for 75% of the total amounts (Yan et al. 2017). According to the relationship between higher alcohols and nitrogen nutrition, combined with the synthesis pathway under different conditions, nitrogen compensation or nitrogen deficiency was considered as an effective means to control the content of higher alcohols (Gutierrez et al. 2013). Therefore, a simple and feasible way to reduce the content of higher alcohols is through nitrogen compensation, in which the nitrogen level in the fermentation system is regulated.

Nitrogen supplementation to the fermentation system not only affects yeast growth and fermentation kinetics but also adjusts and controls the non-volatile and volatile compound composition, including higher alcohols, which show an inverse relationship to the nitrogen concentration (Torrea et al. 2011). Various studies have investigated the effects of nitrogen types on the composition of higher alcohols, optimizing the addition level and process condition of nitrogen compensation (Zhong et al. 2019). An appropriate amount of inorganic nitrogen sources can promote the growth of yeast, while decreasing the content of higher alcohols (Huang et al. 2018; Stéphanie et al. 2018). Ammonium hydrogen phosphate, a food-grade additive, has the best effect on the reduction of the content of higher alcohols, which verifies that the nitrogen source compensation strategy has a certain influence on the formation of higher alcohols (Huang et al. 2018). However, till now, the mechanism of nitrogen compensation in reducing the content of higher alcohol in *S. cerevisiae* has not been studied in CRW in depth.

Proteins are the executors of cell-specific activities and functions, which are responsible for the diversity,

integrity, complexity, functionality, and phenotype of life. Comparative proteomics is regarded as a very powerful tool to reveal biological regulatory mechanisms and comprehend the complementary functions of the whole proteome in a special state and is an important way to evaluate the effects and mechanisms (Hua et al. 2016; Santos et al. 2016). The expression degree and activity of proteins or their interaction with other proteins command-specific functional pattern of organellar, cellular, and organism levels, which can reflect the regulation process of cells with different conditions (Choudhary et al. 2019). Potentially important proteins associated with carbohydrate and nitrogen metabolism and related regulatory proteins may be revealed through comparative proteomic studies. Until now, many studies have investigated and identified a series of genes and proteins associated with higher alcohol synthesis through gene knockout and overexpression (Dickinson 2003; Yoshimoto et al. 2001; Schoondermark-Stolk et al. 2005). However, few studies focused on the mechanism by which the content of higher alcohols is reduced through nitrogen compensation. Therefore, proteomics was used to explore the altered pathways and regulatory effects during the ammonium compensation process to investigate the molecular mechanism of higher alcohol content reduction.

In this study, isobaric tags for relative and absolute quantitation (iTRAQ)-based quantitative proteomic analysis was applied to compare the changes in the relative content of intracellular proteomics in *S. cerevisiae* under different conditions (with or without the addition of ammonium salt). The intracellular proteins that change significantly during the process of ammonium compensation were identified, and then differentially expressed proteins (DEPs) associated with the synthesis metabolism of higher alcohols were analyzed to gain insights into the regulatory mechanism of nitrogen compensation in reducing the content of higher alcohols.

Materials and methods

Materials

Glucose, tryptone, agar, and TEAB were purchased from Sangon Biotech Co. Ltd. (Shanghai, China). Glycerin, $(\text{NH}_4)_2\text{HPO}_4$, urea, acetone, and isopropanol were purchased from Sinopharm Chemical Reagent Co., Ltd. (China). DTT, PMSF, EDTA, and acetonitrile (HPLC grade) were purchased from Shanghai Macklin Biochemical Co., Ltd. (Shanghai, China). Trypsin was obtained from Takara Co., Ltd. (Kyoto, Japan). iTRAQ Reagent 8 Plex One Assay Kit was purchased from SCIEX (Scientific Export).

Strains and culture conditions

The original strain used in this study was fully genotype *Saccharomyces cerevisiae* (*S. cerevisiae*) (available in the School of Food Science and Engineering, Foshan University, China), which was provided by the Food Science and Biotechnology Research Center of JiangNan University.

A single colony of *S. cerevisiae* was picked from a solid slant medium and inoculated into a 250-mL shaking flask that contained 100 mL YPD culture medium. The strains were cultivated at 30 °C at a speed of 120 rpm for 24 h. Subsequently, activated second-generation strain was cultured under the same condition with a 5% inoculum size for 10 h, and OD_{600} was determined after culture dilution.

Experimental treatments

According to our previous research, 200 mg/L $(\text{NH}_4)_2\text{HPO}_4$ is the optimal amount to be added for the reduction of higher alcohols (Zhong et al. 2019). Two groups were set up in this study to explore the mechanism of ammonium compensation: the blank group (no ammonium salt added) and the experimental group (containing a final concentration of 200 mg/L $(\text{NH}_4)_2\text{HPO}_4$), with three parallel samples in each group. $(\text{NH}_4)_2\text{HPO}_4$ was added during inoculation along with *S. cerevisiae*. The critical point of the logarithmic and stationary phase (cultured about 8 h) during fermentation was selected as the time node of intracellular proteome and qPCR study. DEP profiles (comparative proteomics) and mRNA expression levels (real-time quantitative polymerase chain reaction, RT-qPCR) were compared in the control group (without nitrogen feeding) and the experimental group (with nitrogen feeding).

Protein extraction, digestion, and iTRAQ labeling

Cells that were cultured for 8 h to reach the steady state were collected by centrifugation at 25,000×g for 10 min at 4 °C. After supernatant removal, the cell pellets were washed twice with cold deionized water and suspended in a lysis buffer of 10 mM DTT, 2 mM EDTA, and 1 mM PMSF. Cells were disrupted by vortexing and tissue lyser with glass beads (50 Hz, 120 s) to extract the total intracellular proteins, and then the samples were centrifuged at 4 °C, 25,000×g for 20 min. The supernatant was then obtained. The solution was mixed with 10 mM DTT at 56 °C for 1 h, and then IAA was added to reach a final concentration of 55 mM and incubated in the dark for 45 min. The protein solution was placed in a refrigerator at -20 °C for 30 min after being washed 5 times the volume of precooled acetone with vigorous stirring, and then the supernatant was eliminated by centrifugation (25,000×g, 4 °C, 15 min). Precipitation was redissolved with lysis buffer, and insoluble material was

removed by centrifugation at 4 °C, 25,000×g for 15 min; the supernatant was the protein solution. Protein concentrations were determined by a modified Bradford protein assay kit (Sangon Biotech Co. Ltd) with BSA as a standard, as described by Bradford (Bradford 1976).

For each sample, 100 µg protein samples were subjected with 5 µg trypsin digestion at 37 °C overnight, and the enzymatic peptide was desalinated by Strata X column and then vacuumed. Peptides were tagged with iTRAQ tags according to the manufacturer's recommendations. Each sample was dissolved with an addition of 0.5 M TEAB and then transferred to the correct iTRAQ reagent conducted with 50 µL acetone to be incubated at room temperature for 2 h.

Mass spectrometry and proteomic data analysis

C18 column (5 µm 4.6 × 250 mm Gemini C18) was used to desalt the peptides in each sample, and subsequently concentrated by vacuum centrifugation and reconstituted in buffer A (2% acetonitrile, 0.1% formic acid). To conduct the MS experiments on a Q-Exactive HF X (Thermo Scientific, USA) by applying a DDA model, the samples were loaded onto a Trap column to desalt, flowed into the C18 column (75 µm 4.6 × 250 mm) (Thermo Scientific, USA) in buffer A (2% acetonitrile, 0.1% formic acid), and then separated with a linear gradient of buffer B (98% acetonitrile, 0.1% formic acid). The full MS scan (350-1500 m/z) was performed in the positive ion mode at a resolution of 60,000 (at 100 m/z). The top 20 peak which intensity exceeds 10,000 and most intense 2-5 charged ions were selected, and the dynamic exclusion time was set at 30 s.

Data quality control, protein function annotation, and quantitative analysis

Quality control of the data was conducted to determine whether the data were qualified during the search and identification. The final reliable protein identification results could be obtained after all the proteins were screened, with a false discovery rate (FDR) less than 1%. The Gene Ontology (GO), Kyoto Encyclopedia of Genes and Genomes (KEGG), Cluster of Orthologous Groups of proteins (COG), and other databases were used to annotate the identified proteins.

Sequence database search and data analysis

The MaxQuant software suite (version 2.3.02) was used to analyze the MS data, which were searched against the UniProtKB database (Database_info: uniprot_ *Saccharomyces cerevisiae* 190220; Database 27355 sequences). For peptide identification, a mass tolerance of 20 ppm was permitted. This search was conducted with the enzymatic cleavage rule of trypsin with a maximum of two missed cleavage sites allowed. Carbamidomethyl (C),

iTRAQ8plex (N-term), and iTRAQ8plex (K) were defined as fixed modification, while protein methionine oxidation and iTRAQ8plex (Y) were defined as variable modifications. iTRAQ-based quantification was conducted in MaxQuant. Protein quantitation required a protein to contain at least two unique peptides. All the proteins with an FDR less than 1% were then subjected to downstream analysis, including GO, KEGG pathway, GO enrichment analysis, KEGG pathway enrichment analysis, cluster analysis, and subcellular localization analysis. The sequence data of the target proteins were bundled in batches, which were retrieved from the UniProtKB database. The retrieved sequences were searched against the SwissProt database by using NCBI BLAST. The top 10 blast results were retrieved for each query sequence and finally loaded into Blast2GO to analyze the related KEGG pathways.

Real-time quantitative PCR analysis

Total RNA was extracted from the same batch of samples as the proteomic analysis and qualified by using an RNA Extraction Kit (Catalog No. 15596018, Invitrogen TRizol, USA). The concentration and purity of RNA samples were determined through spectrophotometric analysis by considering the absorbance ratio at 260/280 nm. After genomic DNA was removed, RNA (1 µg) was reverse transcribed to cDNA in a 10 µL reaction mixture by using a Bestar® SybrGreen qPCR Master Mix Kit (DBI-2043 Bioscience, Germany). The cDNA was quantified by RT-qPCR reactions on an ABI7300 (Thermo Fisher, USA). Reactions were performed in a 20 µL system that contained 10 µL Bestar® SybrGreen mix, 0.4 µL forward primer (10 µM), 0.4 µL reverse primer (10 µM), 1 µL cDNA, and 8.2 µL ddH₂O. The RT-qPCR procedure was set as follows: initial denaturation at 95 °C for 10 min and followed by 40 cycles of 95 °C for 15 s, 60 °C for 34 s, and 72 °C for 30 s. At the end of the amplification cycle, the melting curves of the PCR amplicons were obtained at 60-98 °C. Relative quantification of the expression level of each gene was normalized according to the β-actin gene (*ACT1*) expression. The primers used in the experiment can be found in the "Additional files" section (Table S1). RT-qPCR was used to confirm the authenticity and accuracy of the proteomic analysis results.

Result and discussion

In our previous study, we found that the content of higher alcohols could be reduced by adding ammonium salt to the medium during the fermentation process of CRW. (NH₄)₂HPO₄ is a suitable inorganic nitrogen source, which leads to a 23.99% decrease in the total higher alcohols from 205.58 to 156.26 mg/L; specifically, isobutyl alcohol, isoamyl alcohol, and β-phenethyl

alcohol decreased by 25.39%, 21.00%, and 12.89%, respectively (Huang et al. 2018; Zhong et al. 2019). These findings proved the feasibility of the nitrogen compensation strategy and confirmed the variety of compensated nitrogen sources. However, the regulatory mechanism of inorganic nitrogen in decreasing the content of higher alcohols was not investigated.

Quality control of the proteome data

In this iTRAQ quantification project, a total of 946,482 spectrums were generated, and 27,973 peptides and 4062 proteins were identified with 1% FDR. Mass spectrometry (MS) data must be subjected to quality control checks, including peptide length distribution, protein mass distribution, unique peptide number, protein coverage, and CV distribution in replicate. A detailed quality control report is shown in Figure S1. iTRAQ technology can identify proteins with different molecular weights, and our result showed that about 12.5% of the identified proteins have a molecular weight of more than 100 kDa, and less than 1% have a molecular weight of 0–10 kDa. In this study, the range of peptide length was 5–25 amino acids, according to the detection limit of MS. The number of protein unique peptides identified in the yeast was correlated to the reliability of the corresponding proteins. More unique peptides correspond to high protein reliability. Of the 4062 identified proteins, 1183 proteins contained one unique peptide segment, and 2879 proteins (70% identified proteins) contained at least two unique peptide segments (Fig. S1C). Therefore, the number of reliable proteins was relatively large, which indicated a high reliability of results. At the same time, 1633 proteins (40.2% of 4062 all identified proteins) had a protein coverage distribution of 0–10%, and 943 proteins (23.2%) had a protein coverage distribution of 10–20%. Other proteins had a protein coverage distribution at 20–100%, accounting for 33.6%, which meant the protein coverage distribution was relatively wide (Fig. S1D). The coefficient of variation (CV) is the ratio of standard deviation to the mean, which was used to evaluate the reproducibility. A lower CV corresponded to good reproducibility. More than 80% of the protein CV was less than 10%, thereby verifying the reliability of the iTRAQ data (Fig. S1E).

Integrative analysis of the global proteomes

On the basis of the large-scale iTRAQ-label comparative proteomic method and statistical filtration (fold change > 1.2, p value < 0.05), about 211 proteins were identified as DEPs in the ammonium compensation group as compared with the control group among the quantified proteins (123 upregulated and 88 downregulated proteins) (Additional file Table S1).

To further understand the functions, all identified proteins and the DEPs between experimental groups and control groups were annotated according to different categories, including GO terms and KEGG pathways. Detailed information of all identified proteins was listed in Additional file Table S2. GO is a major bioinformatics initiative to unify the representation of gene and gene product attributes across all species, and it can flexibly annotate homologous gene and protein sequences in multiple organisms based on biological process, molecular function, and cellular component (Ashburner et al. 2000). In this study, GO annotated 3068 identified proteins, and the GO analysis result of the identified and DEPs was shown in Fig. 1a. Under the biological process category, 2234 identified proteins and 102 DEPs were involved in the metabolic process, and 12 identified proteins and 4 DEPs were involved in the nitrogen utilization. In the molecular function category, 1778 identified proteins and 79 DEPs had binding activities, and 1428 identified proteins and 48 DEPs had catalytic activities. In the cellular component, 2879 identified proteins and 142 DEPs were cell-related proteins; 967 identified proteins and 50 DEPs were membrane related proteins. As can be seen from the bar chart, the GO term enrichment analysis indicated the highest number of DEPs with binding activity, followed by catalytic activity in the molecular function category; the amount of DEPs involved in cell, cell part, and organelle part is the largest in the classification of cell components and those involved in cellular and metabolic processes were the most numerous in *S. cerevisiae*'s biological processes.

The KEGG pathway is a collection of manually drawn pathway maps representing our knowledge on the molecular interaction and reaction networks for many metabolite and signal transduction pathways (Yan et al. 2019). In this study, 1937 proteins were annotated to the KEGG pathway database, and the KEGG analysis result of the identified proteins and DEPs were shown in Fig. 1b. A total of 1935 identified proteins were involved in the metabolism pathway, accounting for 58%, of which 785 identified proteins participated in global and overview maps and 862 of identified proteins (25.8% proteins) were involved in genetic information processing. Moreover, 372, 119, and 40 proteins were involved in cellular processes, environmental information processing, and organismal systems, accounting for 11.1%, 3.6%, and 1.2%, respectively. A total of 148 DEPs were annotated in pathway entries. The amounts of DEPs involved in metabolism accounted for more than half (58.1%), in which global and overview maps accounted for 22.9%, followed by carbohydrate metabolism (10.1%), and amino acid metabolism (6%). The genetic information processing pathway accounted for 20.2%, translation accounted for 9%, and the DEPs involved in cellular

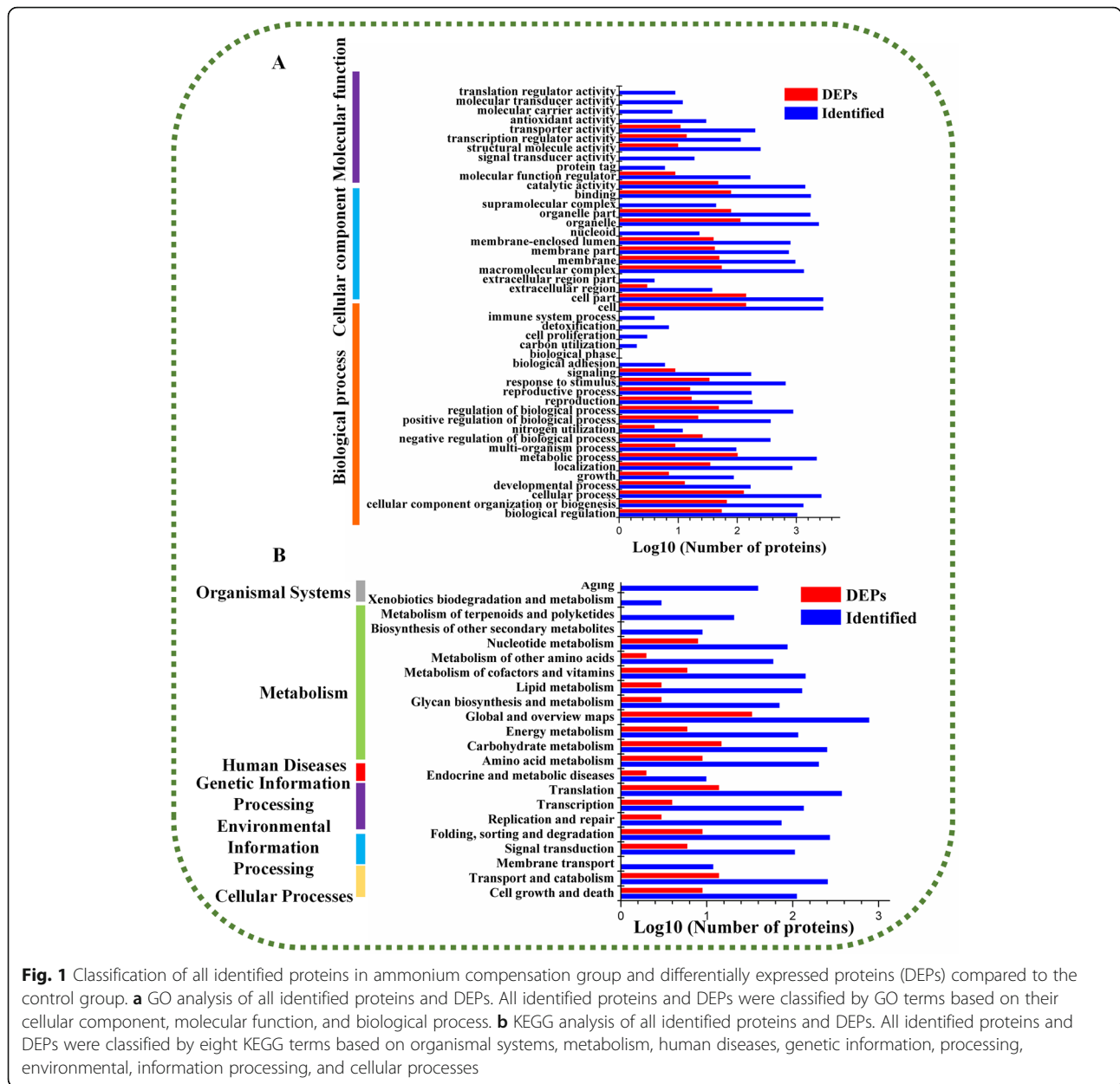


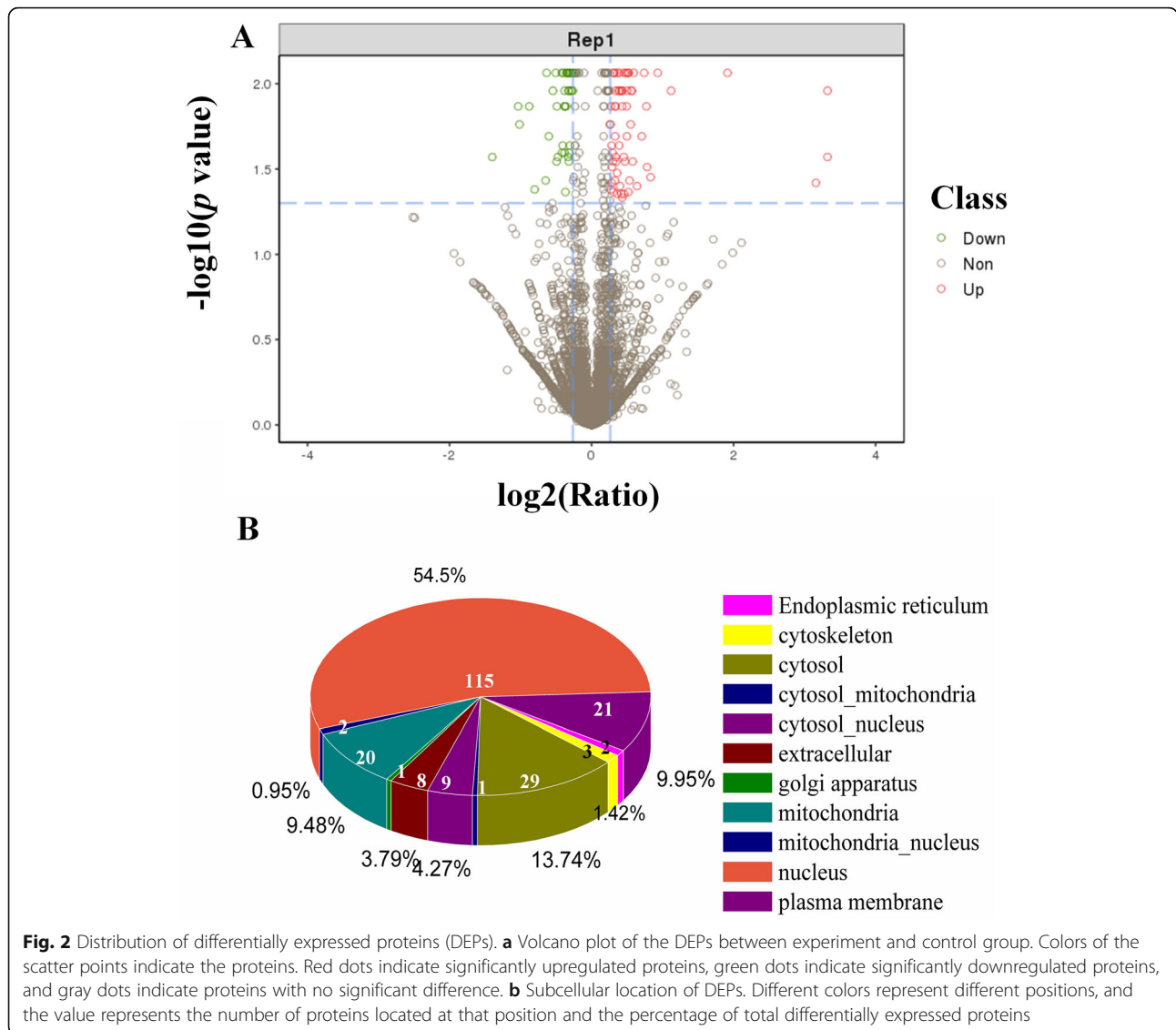
Fig. 1 Classification of all identified proteins in ammonium compensation group and differentially expressed proteins (DEPs) compared to the control group. **a** GO analysis of all identified proteins and DEPs. All identified proteins and DEPs were classified by GO terms based on their cellular component, molecular function, and biological process. **b** KEGG analysis of all identified proteins and DEPs. All identified proteins and DEPs were classified by eight KEGG terms based on organismal systems, metabolism, human diseases, genetic information, processing, environmental, information processing, and cellular processes

processes accounted for 15%. DEPs in *S. cerevisiae* between the experimental group and control group are mainly involved in carbohydrate metabolism and amino acid metabolism.

Protein differential analysis

Figure 2a depicts the volcano plots of identified proteins and differentially expressed proteins. The x-axis showed the logarithm of fold change (base 2), and the negative logarithm of the p value was taken as the y-axis (base 10), representing the probability of the DEPs. A p value less than 0.05 and a fold change more than 1.2 are set as the significant threshold for

differential expression. The red and green dots indicate points of interest that indicate large-magnitude fold changes and high statistical significance, respectively. The red dots mean significantly upregulated proteins that passed the screening threshold, and the green dots mean significantly downregulated proteins. Gray dots are nonsignificant DEPs. The DEPs were grouped based on their subcellular localizations (Fig. 2b). About 11 subcellular components were identified, including 115 nuclear-localized DEPs accounted for 54.5%, 29 cytosol-localized DEPs (13.7%), and 20 mitochondria-localized DEPs (9.48%). Some DEPs in other organelles occurred at multiple locations.

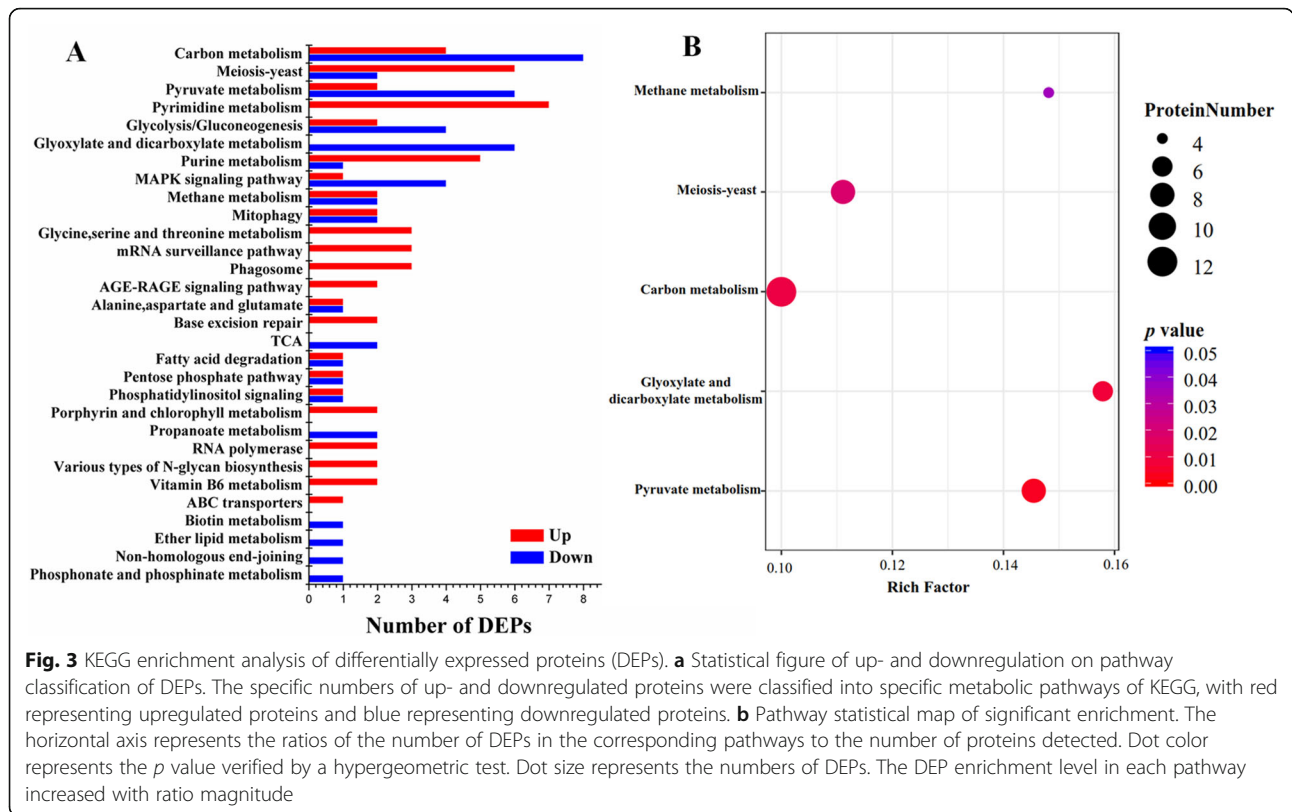


KEGG pathway enrichment analysis of DEPs

KEGG pathway enrichment analysis (El-Dalatony et al. 2019; Yan et al. 2017) was conducted based on the KEGG database for DEP screening, and p value less than 0.05 was set as the standard for significant enrichment of DEPs. The specific number of up- and downregulated DEPs from each pathway annotation item was listed in Fig. 3a. Pyruvate was produced by the glycolysis pathway and then partially entered the TCA cycle. Thus, the differential proteins involved in these three pathways had consistent up and down trends. In addition, multiple differential proteins were found in the amino acid metabolism pathway, such as glycine, serine, and threonine metabolism; alanine, aspartate, and glutamate; and meiosis in yeast.

The metabolic pathway maps for significant enrichment of DEPs were presented in Fig. 3b. In this figure,

the x -axis represented the rich factor, which was the ratio of numbers of DEPs annotated to the corresponding pathway to all identified proteins annotated to this pathway. The enrichment level in each pathway increased with the ratio. The dot size in the figure represented the number of DEPs annotated to this pathway. The p value is related to the intensity of the difference in DEPs. A small p value corresponded to the great difference. The p value for carbon metabolism, glyoxylate and dicarboxylate metabolism, and pyruvate metabolism were all less than 0.01. Therefore, these pathways were significantly enriched for the DEPs. The DEPs involved in the pyruvate metabolism pathway accounted for a larger proportion than others involved in metabolic pathways, and the carbon metabolism pathway annotated the most DEPs. Taken together, these results suggested that the DEPs between the ammonium salt compensation group and



control group were mainly related to metabolic pathways, carbon metabolism, and pathways associated with cell growth.

Differential proteins associated with cell growth

Nitrogen source is a nutritious material that provides nitrogen for the construction of proteins, nucleic acids, and enzymes in cell metabolism. Compared with control, the yeast-specific growth rate increased with the exogenous addition of 200 mg/L $(\text{NH}_4)_2\text{HPO}_4$ during the log phase (Zhong et al. 2019). The main proteins associated with cell growth, which were observed in GO and KEGG enrichment (Fig. 1) were involved in cell growth, meiosis, cellular component organization, or biogenesis (organelle or part, membrane component), growth regulation, and so on. Specific differential proteins included zinc finger protein (Swiss-Prot Accession Number: P32338), mannan endo-1,6-alpha-mannosidase (P36091), transcriptional regulatory protein (P34233), aspartic proteinase precursor (P32329), putative metabolite transport protein (Q12407), and glucose transporter (A6ZT02). The proteomic results supported those of previous studies, which showed that $(\text{NH}_4)_2\text{HPO}_4$ affected growth.

Differential proteins involved in carbohydrate metabolism

In this study, differentially expressed proteins were involved in several pathways, including carbohydrate metabolism (energy), amino acids biosynthesis and metabolism, regulation metabolism, and pathways involved in cell meiosis, cell cycle, growth, and MAPK signaling. The most affected metabolism pathways that were involved in the synthesis of higher alcohols were carbon metabolism and pyruvate metabolism and key amino acid metabolism in *S. cerevisiae*.

In carbon metabolism, two proteins related to the glycolysis were significantly upregulated in the experimental group. One protein was fructose-bisphosphate aldolase (EC:4.1.2.13-P14540) which catalyzed the cleavage reaction from β -D-fructose-1,6-bisphosphate (FBP) to dihydroxyacetone phosphate (DHAP) and glyceraldehyde-3-phosphate (GAP) (Geiger et al. 2019). This aldolase converted carbon six (C6) into two molecule three-carbon (C3) compounds, which marked the step-by-step entry to the second exoenergetic stage of glycolysis. Another upregulated protein was phosphoglycerate mutase (EC:5.4.2.11-Q12008) which converted 3-phosphoglycerate (3-PG) into 2-phosphoglycerate (2-PG). These two enzymes, which were involved in the glycolysis pathway, were all upregulated, which signified that the glycolytic pathway was activated when an

appropriate amount of ammonium salt was added to the system for nitrogen compensation. The identified differentially protein, phosphoenolpyruvate carboxykinase (PEPCK) (EC:4.1.1.49-P10963), was an important enzyme related to a roundabout reaction in the gluconeogenesis pathway. The expression of PEPCK, which converted oxaloacetate into phosphoenolpyruvate (PEP), was significantly downregulated, which might result in the inhibition of the gluconeogenesis pathway.

Interestingly, two different malate dehydrogenases were found as DEPs involved in the TCA cycle and pyruvate metabolism; one protein was upregulated (EC:1.1.1.38-P36013), whereas another was downregulated (EC:1.1.1.37-P22133). The subcellular localization in the cell of the two proteins was examined to distinguish the roles of these two malate dehydrogenase proteins. The results showed that the expression level of the protein in the mitochondria (EC:1.1.1.37-P36013) increased, whereas the level in the cytoplasm (EC:1.1.1.38-P22133) was decreased. The TCA cycle is known to occur in mitochondria. Thus, the upregulation of malate dehydrogenase in the mitochondria indicated that the TCA cycle was proceeding, that is, a certain amount of oxaloacetic acid was accumulated and then, together with acetyl-CoA, the citric acid cycle is completed.

One protein (EC:3.1.1.31-P37262) 6-phosphogluconolactonase, as an important enzyme that converts 6-phosphoglucono- δ -lactone into 6-phosphogluconate in the oxidation stage of the pentose phosphate (PP) pathway (Prabhu and Veeranki 2018), was significantly downregulated. The PP pathway, which was mainly responsible for the reduction of NADPH, ribose-5-phosphate, tetrose, and pentagluconate, was weakened with the decrease in the lactonase enzyme expression level. The expression level of two vital enzymes—namely, isocitrate lyase (EC:4.1.3.1-P28240) and malate synthase (EC:2.3.3.9-P30952 and EC:2.3.3.9-A6ZRW6)—that involved in glyoxylate and dicarboxylate metabolism were all downregulated. The glyoxylic acid cycle is an anaplerotic pathway that used acetyl-CoA as raw material and provided carbon four (C4) acids, and oxaloacetate in the citric acid cycle. The downregulation of all three proteins was probably the consequence of the reduced flux of glyoxylate cycle, that is, acetyl-CoA was directly involved in the TCA cycle without supplementing the oxaloacetate. This phenomenon was consistent with the different regulation of malate dehydrogenase in different parts.

Another downregulated DEP related to the biosynthesis of higher alcohols was alcohol dehydrogenase (EC:1.1.1.1-P00331) in cytoplasmic form, which was directly repressed in the presence of propanol-preferring glucose. The final step in the biosynthesis of

higher alcohols was the reduction of fusel aldehydes into the corresponding higher alcohols. According to the literature, this step was almost catalyzed by ethanol dehydrogenase encoded by *Adh1*, *Adh2*, *Adh3*, *Adh4*, and *Adh5* or formaldehyde dehydrogenase encoded by *Sfa1* (Pires et al. 2014). This downregulation of alcohol dehydrogenase was encoded by *Adh2*, consistent with the reported results.

Differential proteins involved in nitrogen metabolism

One identified DEP, carbamoyl-phosphate synthase (EC:6.3.5.5-P07258, CPS), was an important enzyme related to the nitrogen assimilation pathway (Khoja et al. 2019). CPS, which was identified in this study, referred to the carbamoyl-phosphate synthase II that existed in cytoplasm, which catalyzed the biosynthesis of carbamoyl-phosphate with L-glutamine as a nitrogen source. Carbamoyl-phosphate, which is a high-energy compound, can enter either pyrimidine metabolism or the pathway of arginine biosynthesis. The expression of CPS in cell cultured with nitrogen compensation was increased by 1.2-fold compared with that in cells of the control group. The expression level of CPS positively regulated and promoted the absorption and assimilation of ammonium ions by consuming L-glutamine, which was produced by the glutamate-mediated assimilation pathway and enhanced its metabolic flow in the biosynthesis of pyrimidine and purine.

Interestingly, the expression level of L-serine/L-threonine ammonia lyase (EC:4.3.1.17, 4.3.1.19-Q12008), which catalyzed the conversion of serine/threonine into corresponding pyruvate or 2-oxobutanoate, significantly increased by 1.42-fold compared with that in the control group, which seemed to contradict the experimental phenomena. However, the α -keto acids produced by L-serine or L-threonine deamination had multiple metabolic pathways for utilization and metabolism, which can enter TCA catabolism; synthesize other amino acids such as L-leucine, L-Isoleucine, and L-valine; and even synthesize the corresponding higher alcohols through oxidative decarboxylation. The higher alcohols synthesized by amino acid decarboxylation accounted for only 25% of the total higher alcohols (Huang et al. 2018; Pires et al. 2014), and the catalytic product of this enzyme, α -keto acids, has several metabolic pathways. Therefore, a certain increase in the expression level of L-serine/L-threonine ammonia lyase had little impact on the contribution of higher alcohols.

The expression of 5-aminolevulinic acid synthase (EC:2.3.1.37-P09950), which was an upregulated protein involved in glycine, serine, and threonine, was higher in the experimental group than in the control group. It catalyzed the formation of 5-aminolevulinic acid and CoA from succinyl-CoA and glycine (Bailey et al. 2020), which

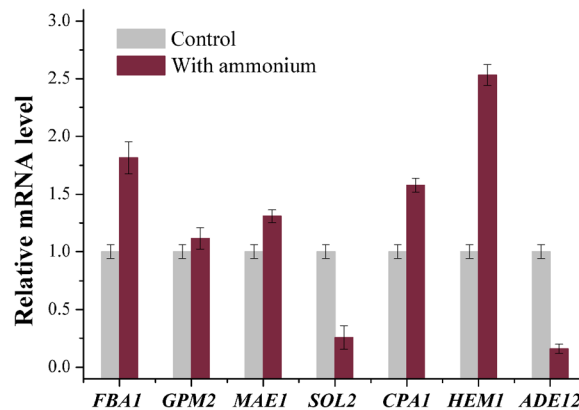


Fig. 4 RT-qPCR analysis of seven selected genes regulated by ammonium compensation in *S. cerevisiae*. *FBA1*, fructose-bisphosphate aldolase encoding gene; *GPM2*, bisphosphoglycerate-dependent phosphoglycerate mutase encoding gene; *MAE1*, malate dehydrogenase encoding gene in the mitochondria; *SOL2*, 6-phosphogluconolactonase encoding gene; *CPA1*, carbamoyl-phosphate synthase encoding gene; *HEMI*, 5-aminolevulinic acid synthase encoding gene; *ADE12*, adenylosuccinate synthetase encoding gene

consumed the succinyl-CoA from the TCA cycle, promoted TCA progression, and facilitated the release of CoA at the same time. Succinyl-CoA is the allosteric inhibitor of the key regulatory enzyme citrate synthase at the beginning of the TCA cycle, and if its content was too high, then it would inhibit the activity of citrate synthase and TCA cycle. Therefore, the upregulated content of 5-aminolevulinic acid synthase was conducive to the smooth progress of the TCA cycle.

Another protein associated with nitrogen metabolism was adenylosuccinate synthetase (EC:6.3.4.4-C8ZG13, AdSS), which is involved in de novo biosynthesis and transamination of purine nucleotide (Galina et al. 2017), and was downregulated. It catalyzed the formation of adenylosuccinate from hypoxanthine nucleotide and aspartic acid. Then, the intermediate product adenylosuccinate splits into adenine nucleotides and fumarate under the action of the cleavage enzyme, realizing the transformation of IMP and AMP.

Validation of gene expression by RT-qPCR

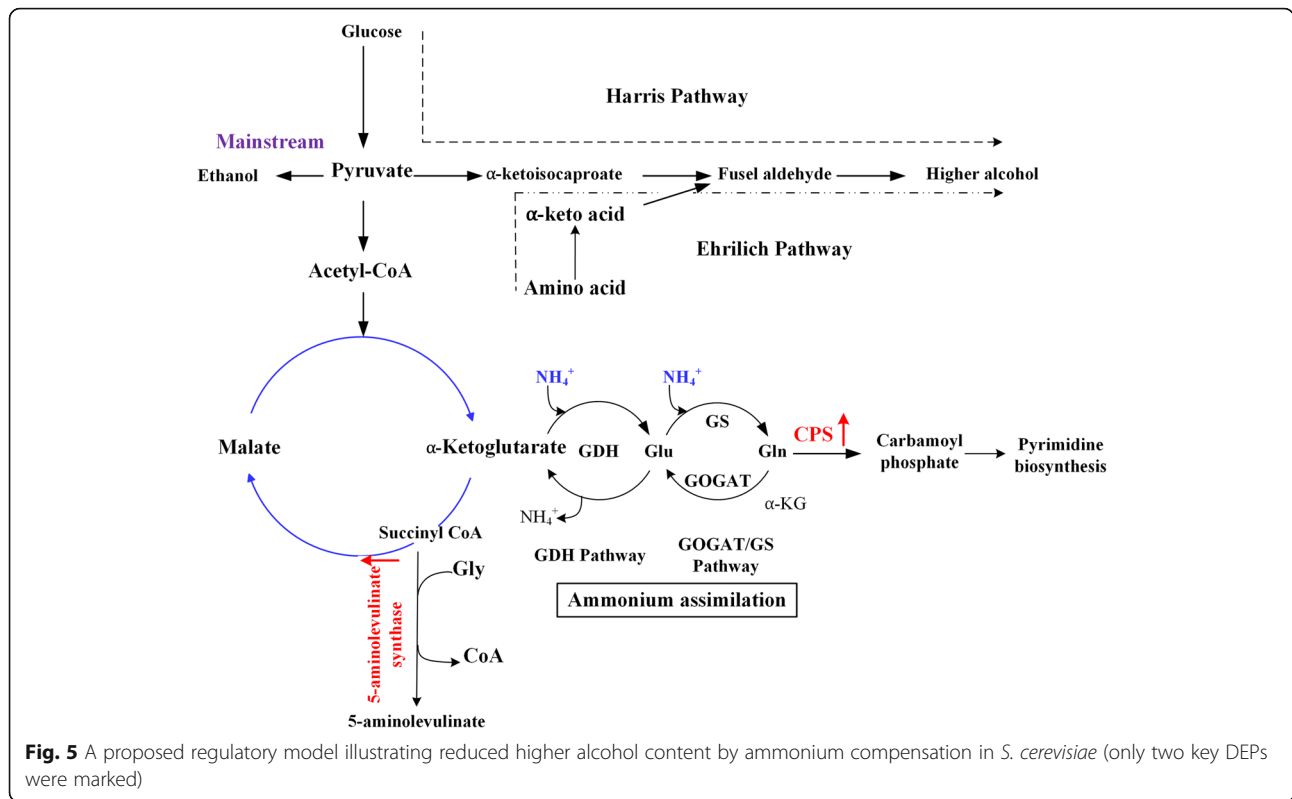
To verify the differential expression levels of some key metabolic genes at mRNA level, RT-qPCR assay was performed. Seven important proteins involved in carbon metabolism and nitrogen metabolism encoding genes were chosen for qPCR analysis with β -actin as the internal reference. The important proteins involved in EMP pathway included fructose-bisphosphate aldolase encoding gene (*FBA1*) and bisphosphoglycerate-dependent phosphoglycerate mutase encoding gene (*GPM2*). The protein involved in the TCA cycle was the malate dehydrogenase encoding gene in the mitochondria (*MAE1*). The protein involved in the PP pathway was selected as the 6-phosphogluconolactonase encoding gene (*SOL2*). The other three proteins were selected as

differential proteins related to nitrogen metabolism according to the proteomic results, such as the carbamoyl-phosphate synthase encoding gene (*CPA1*), the 5-aminolevulinic acid synthase encoding gene (*HEMI*), and the adenylosuccinate synthetase encoding gene (*ADE12*). The expression level of each gene was normalized to the expression of the *act* gene. The expression levels of these selected genes at the mRNA level were basically consistent with the proteomic analyses (Fig. 4). Notably, the fold change of the expression of some proteins at the mRNA level was different from that at the protein level. Take *SOL2* as an example; the mRNA expression level of *SOL2* decreased to 0.25-fold, but it decreased to 0.81-fold of the protein expression level under the condition of ammonium compensation. This phenomenon was normal because no strictly linear relationship existed between genes and proteins, that is, mRNA levels do not correspond to protein levels (Abbott 2001; Fields 2001).

Possible regulatory model for higher alcohol reduction by ammonium compensation

Over the past few decades, proteome analysis has shown outstanding potential in exploring the diversity, complexity, functionality, and phenotype of living organisms, because proteins are often the implementers of specific physiological functions and the mechanisms of change can be interpreted at the protein level. Therefore, to fully understand the effect and mechanism of ammonium compensation on the reduction of higher alcohol content and its association with many other cellular events, a possible approach was to analyze the proteomic analysis of the ammonium compensation group with the control group.

The proteomic comparison analysis results showed that most proteins with a high degree of expression



differences were involved in metabolism, such as carbohydrate, amino acid metabolisms, genetic information process, and cell process, thereby indicating that the significant changes in these metabolic pathways and cellular events were obviously regulated by ammonium compensation. Central carbon metabolism (CCM), including glycolysis, TCA cycle, and PP pathway, was responsible for the production of accessible energy, the composition of important small molecular compounds, and the creation of primary building blocks of other metabolisms for biological life processes (Zhang et al. 2010). However, the regulation of different pathways involved in carbon metabolism was different in *S. cerevisiae* with ammonium compensation. The EMP pathway, a main glycolysis pathway of yeast, is a common metabolic pathway for aerobic or anaerobic respiration. The experimental results showed that the key enzyme expression level of the EMP pathway (fructose-bisphosphate aldolase and phosphoglycerate mutase) was upregulated, indicating that the EMP pathway was activated and the flow rate of this pathway and TCA were enhanced. Other metabolic pathways, such as glyoxylic acid cycle, gluconeogenesis, and PP pathway, were inhibited to some extent.

Based on the synthesis mechanism of higher alcohols, a diagram of possible regulatory mechanisms in response to the reduction of higher alcohol content with ammonium compensation in *S. cerevisiae* was proposed and verified

(Fig. 5). Higher alcohols were synthesized via the Harris and Ehrlich pathways, and ammonium compensation probably affected higher alcohol biosynthesis by fluctuating the flux of TCA and nitrogen metabolism. When ammonium was added to the fermentation system, NH_4^+ rapidly transformed into a form of organic nitrogen, namely, glutamate and glutamine, through the GDH system and the GS/GOGAT ammonium assimilation system, respectively (Roca et al. 2003; Sieg and Trotter 2014). The concentration of α -ketoglutarate was consumed as a result, thus enhancing the TCA pathway metabolic capacity and promoting its continuous progress. Therefore, the metabolism flow and moving directions of pyruvate generated by the EMP pathway were affected. More pyruvate entered the TCA cycle to provide energy and intermediate products for the activities of living organisms, thereby further limiting the conversion of pyruvate into α -ketoisocaproic acid and reducing the conversion flow to the Harris pathway, and finally leading to a decrease in the content of higher alcohols. At the same time, the addition of ammonium salt consumed α -ketoglutarate through the assimilation pathway of ammonium, which competitively inhibited the ammonia transamination of amino acids and reduced the content of higher alcohols produced by the Ehrlich pathway.

Our hypothesis was consistent with the results of proteomic research, which showed that nitrogen assimilation and the concentration of metabolites in the TCA

cycle were involved in the regulation of higher alcohol biosynthesis. These regulation changes at different extents ultimately reduced the content of higher alcohols. Therefore, the synthesis of higher alcohols was coordinated by multiple pathways.

Conclusion

In conclusion, proper ammonium compensation is a promising strategy to reduce the content of higher alcohols in *S. cerevisiae* via adjusting and altering the metabolic flux of pyruvate without affecting the alcohol production rate. Ammonium compensation promotes yeast growth, facilitates glucose consumption, fluctuates TCA cycles and amino acid metabolism, channels pyruvate flux into the TCA cycle, and decreases the synthesis of α -ketoisocaproic acid and the metabolic flux of the Harris pathway. These findings may shed light on the molecular mechanism of higher alcohol synthesis in *S. cerevisiae*. The up- or downregulated proteins could serve as targeted sites for genetic engineering or genome editing to decrease the content of higher alcohols.

Supplementary Information

The online version contains supplementary material available at <https://doi.org/10.1186/s13213-020-01611-7>.

Additional file 1: Table S1. The detail information of DEPs.

Additional file 2: Table S2. The detail information of all identified proteins.

Additional file 3: Figure S1. Distribution of protein mass (A), peptide length (B), unique peptide number (C), protein coverage (D), and CV distribution in replicate (E). **Table S1.** The primers used in the experiment.

Acknowledgements

Not applicable.

Authors' contributions

Guidong Huang designed the experiments and revised the manuscript. Hong Ren analyzed the data and prepared the manuscript. Ali Wang contributed to the manuscript revision. Xianfeng Zhong reviewed and approved the final manuscript, and other authors prepared the samples and performed the experiments. The author(s) read and approved the final manuscript.

Funding

This work was supported by the National Natural Science Foundation of China (No. 31660459), the Natural Science Foundation of Guangdong Province (No. 2018A0303130275; No. 2020A1515011444).

Availability of data and materials

All data included in this study are available upon request by contact with the corresponding author.

Ethics approval and consent to participate

This article does not contain any studies with human participants or animals.

Consent for publication

Not applicable.

Competing interests

The authors declare that they have no conflict of interest.

Author details

¹Department of Food Science, Foshan University, Foshan 528231, China. ²Guangdong Engineering Research Center for Traditional Fermented Food, Foshan 528231, China. ³Guangdong Engineering Research Center for Safety Control of Food Circulation, Foshan 528231, China. ⁴Foshan Engineering Research Center for Brewing Technology, Foshan 528231, China. ⁵Foshan Engineering Research Center for Agricultural Bio-manufacturing, Foshan 528231, China.

Received: 19 August 2020 Accepted: 20 November 2020

Published online: 14 January 2021

References

- Abbott A (2001) And now for the proteome. *Nature* 409(6822):747
- Ashburner M, Ball CA, Blake JA, Botstein D, Butler H, Cherry JM, Davis AP, Dolinski K, Dwight SS, Eppig JT, Harris MA, Hill DP, Issel-Tarver L, Kasarskis A, Lewis S, Matese JC, Richardson JE, Martin R, Rubin GM, Sherlock G (2000) Gene Ontology: tool for the unification of biology. *Nat Genet* 25:25–29
- Bailey HJ, Bezerra GA, Marcerio JR, Padhi S, Foster WR, Rembeza E, Roy A, Bishop DF, Desnick RJ, Bulusu G, Dailey HA Jr, Yue WW (2020) Human aminolevulinatase synthase structure reveals a eukaryotic-specific autoinhibitory loop regulating substrate binding and product release. *Nat Commun* 11:2813–2825
- Bradford MM (1976) A rapid and sensitive method for the quantitation of microgram quantities of protein utilizing the principle of protein-dye binding. *Anal Biochem* 72:248–254
- Choudhary J, Singh S, Tiwari R, Goel R, Nain L (2019) An iTRAQ based comparative proteomic profiling of thermotolerant *Saccharomyces cerevisiae* JRC6 in response to high temperature fermentation. *Curr Proteomic* 16:289–296
- Dickinson JR (2003) The catabolism of amino acids to long chain and complex alcohols in *Saccharomyces cerevisiae*. *J Biol Chem* 278:8028–8034
- El-Dalatony MM, Saha S, Govindwar SP, Abou-Shanab RAI, Jeon B-H (2019) Biological conversion of amino acids to higher alcohols. *Trends Biotechnol* 37:855–869
- Fang C, Du H, Jia W, Xu Y (2018) Compositional differences and similarities between typical Chinese Baijiu and western liquor as revealed by mass spectrometry-based metabolomics. *Metabolites* 9(1):2
- Fields S (2001) Proteomics in genomeland. *Science* 291(5507):1221–1224
- Galina L, Dalberto PF, Martinelli LKB, Roth CD, Pinto AFM, Villela AD, Bizarro CV, Machado P, Timmers L, de Souza ON, Carvalho EMD, Basso LA, Santos DS (2017) Biochemical, thermodynamic and structural studies of recombinant homotetrameric adenylosuccinate lyase from *Leishmania braziliensis*. *RSC Adv* 7:54347–54360
- Gao X, Li B, Mei J (2018) Research progress in active components and functional properties of yellow rice wine. *Brewing Technol* 1:91–96
- Geiger J, Doelker R, Salo S, Roitsch T, Dalgaard LT (2019) Physiological phenotyping of mammalian cell lines by enzymatic activity fingerprinting of key carbohydrate metabolic enzymes: a pilot and feasibility study. *BMC Res Notes* 12:682–688
- Gutierrez A, Chiva R, Beltran G, Mas A, Guillamon JM (2013) Biomarkers for detecting nitrogen deficiency during alcoholic fermentation in different commercial wine yeast strains. *Food Microbiol* 34:227–237
- Hazelwood LA, Daran J-M, Maris AJ, Pronk JT, Dickinson JR (2008) The Ehrlich pathway for fusel alcohol production: a century of research on *Saccharomyces cerevisiae* metabolism. *Appl Environ Microbiol* 74:2259–2266
- Hua Y, Wang S, Liu Z, Liu X, Zou L, Gu W, Hou Y, Ma Y, Luo Y, Liu J (2016) iTRAQ-based quantitative proteomic analysis of cultivated *Pseudostellaria heterophylla* and its wild-type. *J Proteomics* 139:13–25
- Huang G, Shanshan XU, Liu H, Mao J, Zukang FU, Sun G, Zhou Z (2018) Selected inorganic nitrogen in reducing the contents of higher alcohols from Chinese rice wine. *J Food Sci Biotechnol* 37:82–87
- Khoja S, Nitzahn M, Truong B, Lambert J, Willis B, Allegri G, Rufenacht V, Haberle J, Lipschutz GS (2019) A constitutive knockout of murine carbamoyl phosphate synthetase 1 results in death with marked hyperglutaminemia and hyperammonemia. *J Inher Metab Dis* 42:1044–1053
- Longo R, Carew A, Sawyer S et al (2020) A review on the aroma composition of Vitis vinifera L. Pinot noir wines: origins and influencing factors. *Crit Rev Food Sci Nutr*. <https://doi.org/10.1080/10408398.2020.1762535>
- Pires EJ, Teixeira JA, Brányik T, Vicente AA (2014) Yeast: the soul of beer's aroma—a review of flavour-active esters and higher alcohols produced by the brewing yeast. *Appl Microbiol Biotechnol* 98:1937–1949

- Prabhu AA, Veeranki VD (2018) Metabolic engineering of *Pichia pastoris* GS115 for enhanced pentose phosphate pathway (PPP) flux toward recombinant human interferon gamma (hIFN-gamma) production. *Mol Biol Rep* 45:961–972
- Roca C, Nielsen J, Olsson L (2003) Metabolic engineering of ammonium assimilation in xylose-fermenting *Saccharomyces cerevisiae* improves ethanol production. *Appl Environ Microbiol* 69:4732–4736
- Rollero S, Bloem A, Camarasa C, Sanchez I, Ortiz-Julien A, Sablayrolles JM, Dequin S, Mouret JR (2015) Combined effects of nutrients and temperature on the production of fermentative aromas by *Saccharomyces cerevisiae* during wine fermentation. *Appl Microbiol Biotechnol* 99:2291–2304
- Santos RM, Nogueira FCS, Brasil AA, Carvalho PC, Leprevost FV, Domont GB, Eleutherio ECA (2016) Quantitative proteomic analysis of the *Saccharomyces cerevisiae* industrial strains CAT-1 and PE-2. *J Proteomics* 151:114–121
- Schoondermark-Stolk SA, Maria T, John C, ter Schure EG, Theo VC, Verkleij AJ, Johannes B (2005) Bat2p is essential in *Saccharomyces cerevisiae* for fusel alcohol production on the non-fermentable carbon source ethanol. *FEMS Yeast Res* 5:757–766
- Sieg AG, Trotter PJ (2014) Differential contribution of the proline and glutamine pathways to glutamate biosynthesis and nitrogen assimilation in yeast lacking glutamate dehydrogenase. *Microbiol Res* 169:709–716
- Stéphanie R, Audrey B, Anne O-J, Carole C, Benoit D (2018) Fermentation performances and aroma production of non-conventional wine yeasts are influenced by nitrogen preferences. *FEMS Yeast Res* 18:1–11
- Stribny J, Querol A, Pérez-Torrado R (2016) Differences in enzymatic properties of the *Saccharomyces kudriavzevii* and *Saccharomyces uvarum* alcohol acetyltransferases and their impact on aroma-active compounds production. *Front Microbiol* 7:1–13
- Sun H, Liu S, Mao J et al (2020) New insights into the impacts of huangjiu components on intoxication. *Food Chem* 317:126420
- Torrea D, Varela C, Ugliano M, Ancin-Azpilicueta C, Francis IL, Henschke PA (2011) Comparison of inorganic and organic nitrogen supplementation of grape juice -effect on volatile composition and aroma profile of a Chardonnay wine fermented with *Saccharomyces cerevisiae* yeast. *Food Chem* 127:1072–1083
- Wang J, Yuan CJ, Gao XL, Kang YL, Huang MQ, Wu JH, Liu YP, Zhang JL, Li HH, Zhang YY (2020) Characterization of key aroma compounds in Huangjiu from northern China by sensory-directed flavor analysis. *Food Res Int* 134:109238
- Xie GF (2008) Functional constituents and health function of Chinese rice wine. *Liquor Making* 35:14–15
- Xie J, Tian X-F, He S-G, Wei Y-L, Peng B, Wu Z-Q (2018) Evaluating the intoxicating degree of liquor products with combinations of fusel alcohols, acids, and esters. *Molecules* 23:1–12
- Yan N, Du Y, Liu X, Chu M, Shi J, Zhang H, Liu Y, Zhang Z (2019) A comparative UHPLC-QqQ-MS-based metabolomics approach for evaluating Chinese and North American wild rice. *Food Chem* 275:618–627
- Yan N, Du Y, Liu X, Zhang H, Liu Y, Shi J, Xue SJ, Zhang Z (2017) Analyses of effects of α -cembatrien-diol on cell morphology and transcriptome of *Valsa mali* var. *mali*. *Food Chem* 214:110–118
- Yoshimoto H, Fukushige T, Yonezawa T, Sakai Y, Okawa K, Iwamatsu A, Sone H, Tamai Y (2001) Pyruvate decarboxylase encoded by the *PDC1* gene contributes, at least partially, to the decarboxylation of α -ketoisocaproate for isoamyl alcohol formation in *Saccharomyces cerevisiae*. *J Biosci Bioeng* 92:83–85
- Yuan N, Guan GK, Wan Z, Xia PY, Liu Y, Wang T, Chen YF, Zheng N, Han QY (2018) Application of modified yeast in reducing higher alcohols content in yellow rice wine. *Liquor Making Sci Technol* 8(290):85–88
- Zhang N, Gur A, Gibon Y, Sulpice R, Flint-Garcia S, McMullen MD, Stitt M, Buckler ES (2010) Genetic analysis of central carbon metabolism unveils an amino acid substitution that alters maize NAD-dependent isocitrate dehydrogenase activity. *Plos One* 5:1–10
- Zheng N, Jiang S, He Y, Chen Y, Zhang C, Guo X, Ma L, Xiao D (2020) Production of low-alcohol Huangjiu with improved acidity and reduced levels of higher alcohols by fermentation with scarless *ALD6* overexpression yeast. *Food Chem* 321:1–7
- Zhong X, Wang A, Zhang Y, Wu Z, Wen H (2019) Reducing higher alcohols by nitrogen compensation during fermentation of Chinese rice wine. *Food Sci Biotechnol* 29:805–816

Publisher's Note

Springer Nature remains neutral with regard to jurisdictional claims in published maps and institutional affiliations.

Ready to submit your research? Choose BMC and benefit from:

- fast, convenient online submission
- thorough peer review by experienced researchers in your field
- rapid publication on acceptance
- support for research data, including large and complex data types
- gold Open Access which fosters wider collaboration and increased citations
- maximum visibility for your research: over 100M website views per year

At BMC, research is always in progress.

Learn more [biomedcentral.com/submissions](https://www.biomedcentral.com/submissions)

